Nanoscale

Accepted Manuscript

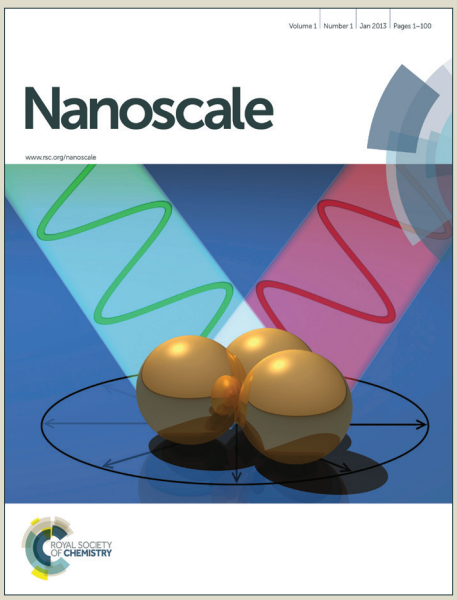

This is an *Accepted Manuscript*, which has been through the Royal Society of Chemistry peer review process and has been accepted for publication.

Accepted Manuscripts are published online shortly after acceptance, before technical editing, formatting and proof reading. Using this free service, authors can make their results available to the community, in citable form, before we publish the edited article. We will replace this *Accepted Manuscript* with the edited and formatted *Advance Article* as soon as it is available.

You can find more information about *Accepted Manuscripts* in the Information for Authors.

Please note that technical editing may introduce minor changes to the text and/or graphics, which may alter content. The journal's standard Terms & Conditions and the Ethical guidelines still apply. In no event shall the Royal Society of Chemistry be held responsible for any errors or omissions in this *Accepted Manuscript* or any consequences arising from the use of any information it contains.

ROYAL SOCIETY OF CHEMISTRY

www.rsc.org/nanoscale

Please do not adjust margins

Nanoscale

PAPER

Multicolor Fluorescent Graphene Quantum Dots Colorimetrically Responsive to All-pH and Wide Temperature Range

Received 00th January 20xx,
Accepted 00th January 20xx

DOI: 10.1039/x0xx00000x

www.rsc.org/

Fanglong Yuan,[a] Ling Ding,[a] Yunchao Li,[a] Xiaohong Li,[a] Louzhen Fan,*[a] Shixin Zhou,[b] Decai Fang,[a] and Shihe Yang[c]

Smart functional nanomaterials colorimetrically responsive to all-pH and a wide temperature range are urgently needed due to their widespread applications in biotechnology, drug delivery, diagnosis and optical sensing. Although graphene quantum dots possess remarkable advantages in biological applications, they are only stable in neutral or weak acidic solutions, and strong acidic or alkaline conditions invariably suppress or diminish the fluorescence intensity. Herein, we report a new type of water-soluble, multicolor fluorescent graphene quantum dots which are responsive to all-pH from 1 to 14 with the naked eye. The synthesis was accomplished by electrolysis of graphite rod, followed by refluxing in a concentrated nitric and sulfuric acid mixed solution. We demonstrate novel red fluorescence of quinone structures transformed from the lactone structures in strong alkaline condition. The fluorescence of resulting graphene quantum dots was also found to be responsive to the temperature changes, demonstrating the great potential as a dual probe of pH and temperature in complicated environments such as biological media.

Introduction

Intelligent, stimulus-responsive functional materials have drawn great interest in the last few years owing to the desire to control complexity and to create systems that adapt or respond to the environment such as pH, temperature, chemical or mechanical stress.[1] pH papers as classic intelligent responsive materials have been widely used since they can rapidly and easily determine narrow pH ranges in numerous applications by recognizing different colors with the naked eye. Great efforts have been taken, ranging from the initial synthesis to the optical characterization, in the hope of finding luminescent intelligent materials that show highly sensitive response to environment factors.

Graphene quantum dots (GQDs), a new type of quantum dot system, have drawn great excitement for their remarkably advantages in biological applications owing to their stable photoluminescence (PL), excellent biocompatibility and low cytotoxicity.[2-11] There has been also great interest in using GQDs as nanoscale probes and sensors in biological electronics and optical devices because these properties of GQDs are extremely sensitive to the surrounding environments such as pH value and temperature. But up to now, GQDs are found to be only stable in neutral or weak acidic solution, while strong acidic or alkaline conditions always result in reduced PL intensity.[12,13] The PL of GQDs was found to be quenched and recovered by varying pH value between 13 and 1 with almost no shift in fluorescence emission peak.[14-16] Yang et al. reported that the PL peak of GQDs showed blue shift as the pH value increases.[17] GQDs that prepared using a two-step cutting process from graphene oxides (GOs) showed a very slight red shift about 10 nm in fluorescence peak by changing pH between 1 and 10 due to the protonation or deprotonation of the functional groups.[18] It is critically important but remains challenging to prepare GQDs that chromatically respond to full pH-range, specially highly acidic and alkaline condition.

Herein, we report on a novel multicolor fluorescent (MCF) GQDs, whose colorimetric change in different pH from 1 to 14 can be easily perceived with the naked eye under ultraviolet lamp. A new quinone structure in GQDs transformed from lactone structure in strong alkaline condition found for the first time is responsible for the red fluorescence in strong alkaline condition. More importantly, these MCF GQDs simultaneously respond to temperature in a wide range, making them an ideal candidate of dual sensing probe for sensitive reversible fluorescence response to pH value and temperature for bioimaging applications.

Experimental section

Reagents and materials

Graphite rods (Shanghai Carbon Co. Ltd), tetrabutylammonium perchlorate (TBAP) (Lark wei technology Co. Ltd), dimethylsulfoxide (DMSO), C_2H_6O, concentrated sulphuric acid (98%), concentrated nitric acid (68%), NaOH, Na_2CO_3, citric acid, KH_2PO_4, $Na_2B_4O_7$, Tris, KCl,

[a]Department of Chemistry, Beijing Normal University, Beijing, 100875, China. E-mail: lzfan@bnu.edu.cn
[b]Department of Cell Biology, School of Basic Medicine, Peking University Health Science Center, Beijing, 100191, China
[c]Department of Chemistry, The Hong Kong University of Science and Technology, Clear Water Bay, Kowloon, Hong Kong, China

This journal is © The Royal Society of Chemistry 2015

Nanoscale Accepted Manuscript

Formatted: Font color: Black

Please do not adjust margins

HCl (68%) were all bought from Beijing Chemical Works. All solvents and reagents were purchased and used without further purification.

Synthesis of MCF GQDs

The thin and small sized graphenes were prepared through an electrochemical approach performed on HDV-7C transistor potentiostat, with graphite rod as working electrode inserted into 5 ml DMSO solution which contained 0.01 M TBAP, paralleled to a Pt foil used as counter electrode. After electrolysis of graphite rod for 3 h with cathode current about 10 mA, the resulting black suspension was washed with ethanol and then centrifuged for several times to remove TBAP and DMSO. Finally, it was dried at 75 °C in the oven for one day. The graphenes obtained above (0.1 g) were first added into a 50 ml flask, and then 5 ml concentrated nitric acid, 10 ml concentrated sulfuric acid was slowly added under ice water bath condition. The mixture was heated at 80 °C in the oil bath under magnetic stirring and reflux condensation for 24 h. After the reaction, the reactors were cooled to room temperature naturally, then the solution was diluted with deionized water, neutralized by sodium carbonate and the supernatant was collected by centrifugation. Finally, the solution was subjected to dialysis in order to obtain the MCF GQDs.

Universal buffer solution

The pH response experiment was carried out in universal buffer solution. Universal buffer solution (0.1 M citric acid, 0.1 M KH_2PO_4, 0.1 M $Na_2B_4O_7$, 0.1 M Tris, 0.1 M KCl) was adjusted to corresponding pH using 37% HCl solution and saturated NaOH solution determined by the pH meter. The concentration of universal buffer solution finally used was 10 mM.

Quantum yields (QY) measurements

The QY was determined by the slope method using the reference of Rhodamine 6G, i.e., comparing the integrated photoluminescence intensity and the absorbance [several values (< 0.1 at the excitation wavelength) gave the curve] of the samples with those of the references. The GQDs and Rhodamine 6G were dissolved in water and ethanol, respectively. The following equation was used:

$$\Phi_X = \Phi_{ST}\left(\frac{m_X}{m_{ST}}\right)\left(\frac{\eta_X^2}{\eta_{ST}^2}\right)$$

Where Φ is the QY, m is the slope determined by the curves and η is the refractive index. The subscript "ST" refers to the standards and "X" refers to the unknown samples. Here, η_x/η_{st}=1.33/1.36=0.9779, Φ_{ST}=0.95. The QY of MCF GQDs was determined to be about 9.1 % in neutral condition.

Characterization method

Atomic force microscopic (AFM) images were taken with MultiMode V SPM (VEECO). A JEOL JEM 2100 transmission electron microscope (TEM) was used to investigate the morphologies of the GQDs. X-ray diffraction (XRD) patterns were carried out by an X-ray diffraction using Cu-Ka radiation (XRD, PANalytical X'Pert Pro MPD). Absorption spectra were recorded on UV-2450 spectrophotometry. The fluorescence spectra of MCF GQDs at different pH solutions were measured on a PerkinElmer-LS55 luminescence spectrometer with slit width at 2.5-2.5 nm. The photographs were taken with camera (Nikon, D7200) under UV light excited at 365 nm (UV light: SPECTROLINE, ENF-280C/FBE, 8W). The FT-IR spectra were measured using a Nicolet 380 spectrograph. X-ray photoelectron spectroscopy (XPS) was performed with an ESCALab220i-XL electron spectrometer from VG Scientific using 300 W Al Ka radiation. The Raman spectrum was measured using Laser Confocal Micro-Raman Spectroscopy (LabRAM Aramis). The Zeta potential and DLS size of MCF GQDs in different pH solutions were performed on ZetaPlus Zeta Potential Analyzer (brookhaven, 100-240V, 50/60 Hz). The fluorescence lifetimes of MCF GQDs were performed with a time-correlated single-photon counting (TCSPC) system under right-angle sample geometry. A 460 nm picosecond diode laser (Edinburgh Instruments EPL375, repetition rate 2 MHz) was used to excite MCF GQDs in different pH solutions.

Cellular imaging for pH and temperature in living cells

The Human cervix carcinoma (Hela) cells were chosen to assess the fluorescence properties of MCF GQDs. After incubating for 24 h (37 °C, 5% CO_2, in Dulbecco's modified Eagle's medium (DMEM)), the culture medium was replaced by DMEM high glucose containing the MCF GQDs at predetermined pH value or temperature and further incubated for 2 h at 37 °C. In order to equilibrate intracellular pH values, 10^{-6} g/ml nigericin and Britton-Robinson buffer solution with pH at 5, 7, 9 was added for 30 min to allow a rapid exchange of K^+ and H^+ which resulted in a rapid equilibration of external and internal pH values. Finally, the Hela cells were analyzed by confocal laser scanning microscopy. For the temperature sensitive cell imaging, the Hela cells were analyzed by confocal laser scanning microscopy at predetermined temperature controlled by temperature controlled heater.

Results and discussion

MCF GQDs are prepared by electrolysis of graphite rod in 0.01 M tetrabutylammonium perchlorate (TBAP) dimethylsulfoxide (DMSO) solution with cathode current about 10 mA for 3 h, which is followed by refluxing the resulting powder in concentrated nitric and sulfuric acid mixed solution at 80 °C for 24 h. After diluted with deionized water, neutralized by sodium carbonate and finally subjected to dialysis in deionized water, a yellow transparent solution could be obtained as shown in Figure 1a (pH=7).

Interestingly, upon varying the pH value from 1 to 14, as prepared MCF GQDs solution displays a clear color appearance change from light yellow to brown and to red as shown in Figure 1a. Moreover, the fluorescence of MCF GQDs chromatically responds to the pH value under UV light, which is easily perceived with the naked eye. Figure 1b shows the

Nanoscale Accepted Manuscript

 This journal is © The Royal Society of Chemistry 2015

Please do not adjust margins

photograph of the MCF GQDs with the pH value from 1 to 14, which is recorded by a digital camera under illumination with UV light. A gradual color change from yellow-green, yellow, yellow-orange, orange to red was clearly observed (Figure S1 in the supporting information). This pH-chromatism of MCF GQDs is highly reversible as pH of the solution is cycled in a wide range.

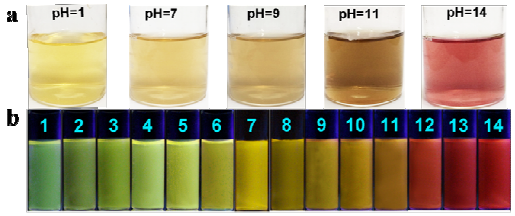

Figure. 1 Photographs showing color appearance (a) and fluorescence images under UV light (excited at 365 nm) (b) of the MCF GQDs in universal buffer solution at different pH values.

Transmission electron microscopy (TEM) and atomic force microscope (AFM) (Figure 2) images reveal that MCF GQDs are uniform in size with an average diameter about 10.6 nm (Figure S2), topographic height below 1.4 nm and the lattice spacing of 0.21 nm (in-plane lattice spacing of graphene[19]), indicating that most of the MCF GQDs consist of ca. 1-3 graphene layers. Raman and XRD spectra (Figure S3) demonstrate that there are numerous defects on MCF GQDs.[20,21]

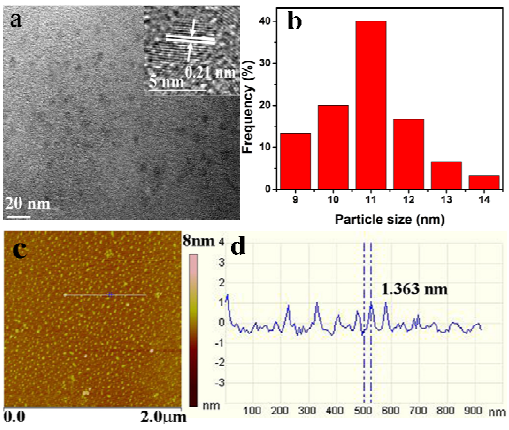

Figure. 2 TEM (a) and HRTEM (inset) images and the corresponding size distribution (b) of MCF GQDs. AFM (c) and corresponding height image (d) of MCF GQDs.

The most distinctive feature which sets them apart from other previously reported GQDs is the specific chromatically responsive to the pH value from 1 to 14. A detailed PL investigation was carried out with different pH solutions (Figure S4-S6 and Table S1). As shown in Figure 3a, there are obviously two parts in the normalized PL spectra. For the first part, the PL peak position red shifts monotonically from 522 to 575 nm as the pH value increases from 1 to 11 (excited at 365 nm), which should most likely arise from the deprotonation of oxygen containing functional groups, such as epoxy, hydroxyl and carboxyl groups, and the consequent electrostatic doping/charging of the GQDs and shifting of the Fermi level.[22-24] The second part reveals essentially a different phenomenon from the first part. When the pH is higher than 11, the second PL part displays an markedly strong emission centered at about 625 nm (pH 12 : 619 nm, pH 13 : 623 nm, pH 14 : 625 nm) corresponding to red fluorescence color. Owing to the overlap with the spectrum in the first part, the left side of the second part exhibits decreased emission intensity and the blue-shift emission peak from 536 nm (pH 12) to 520 nm (pH 13) and then to 493 nm (pH 14). The red fluorescence emission peak remains almost unshifted with excitation wavelengths from 360 to 560 nm (Figure S7), indicating the PL origin here is obviously dissimilar to that of the first part and other GQDs with excitation wavelength dependent PL.[13-17] Comparing the absorption spectra of MCF GQDs in the solution of pH from 1 to 14 (Figure 3b, S8), it can be seen that an increase of pH from 1 to 11 induces a red shift of the maximum absorption from 292 to 316 nm, but a notable new wide absorption peak at about 520 to 560 nm is observed from pH 12 to 14. It is quite evident that a new fluorophore group in MCF GQDs is responsible for the red fluorescence color.

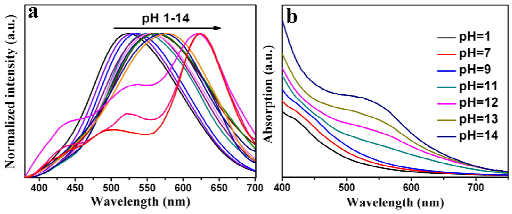

Figure. 3 Normalized fluorescence spectra excited at 365 nm (a) and UV-vis absorption spectra (b) of MCF GQDs in universal buffer solution at different pH values.

Efforts were made to characterize the origin of red fluorescence emission of MCF GQDs solution at pH 12 to 14. The FTIR spectrum of MCF GQDs in neutral condition is revealed in Figure 4a, where the stretching vibration bands of O–H, C=O and C=C are observed at 3435, 1728 and 1620 cm^{-1}, respectively. The strong band at 1427 cm^{-1} is attributed to the bending vibration of O-H. It is worth noting that two typical bands at 1260 and 1140 cm^{-1} are ascribed to the asymmetric stretching vibration band of C=O and stretching vibration band of C-O-C in lactone structure.[25] The epoxy group (C-O-C) stretching vibration band at 1062 cm^{-1} shows smaller wavenumber compared to the stretching vibration band of C-O-C in lactone structure. Further support of the lactone structure is demonstrated by XPS spectrum in neutral condition (Figure 4b and S9). Except the highest peak at 284.8

Formatted: Font color: Black

Nanoscale Accepted Manuscript

Please do not adjust margins

eV corresponding to the C-C group, the peak at 288.8 eV corresponding to the O=C-O group confirms the presence of lactone structure with a relatively high amount. Other groups such as C-OH (286.0 eV), C-O-C (286.7 eV), C=O (287.6 eV) are also observed clearly, in good agreement with the results of FTIR spectrum.[26-28]

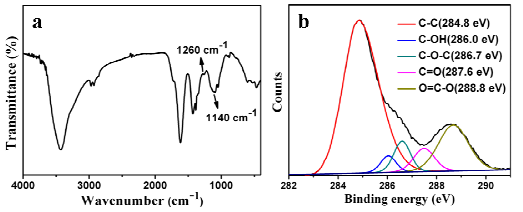

Figure. 4 FTIR (a) and C1s XPS (b) spectra of MCF GQDs in neutral condition.

The lactone groups and color appearance change are reminiscent of the structure of phenolphthalein whose appearance color changes from colorless to red when the solution changes to alkaline condition, which is caused by the transforming of the lactone structure into quinone structure (Figure S10a). Correspondingly, the new absorption peak at 520-560 nm of MCF GQDs from pH 12 to 14 is in consistence with the absorption peak at 550 nm of quinone structure of phenolphthalein transformed from the lactone structure in alkaline condition (Figure S10b). The transformation of the quinone structure from lactone structure was further demonstrated by the FTIR and XPS spectra of MCF GQDs in strong alkaline condition of pH 13 (as shown in Figure 5). It could be seen that the two typical bands at 1260 and 1140 cm^{-1} for lactone structure of MCF GQDs in neutral condition disappeared (Figure 5a), while a new wide band at 1655 cm^{-1} appeared in strong alkaline condition, which could be ascribed to the stretching vibration band of C=O in quinone structure. Compared with XPS spectra of MCF GQDs in neutral condition, the intensity of C1s spectra in strong alkaline condition increased at 288.1 eV (C=O group) and decreased at 286.6 eV (C-O-C group) (Figure 5b), which further demonstrates the transformation of the lactone structure to quinone structure. Moreover, the red shift of the peak from 288.8 to 289.1 eV indicates the transformation of O=C-O group of lactone structure to COO^- group.[25]

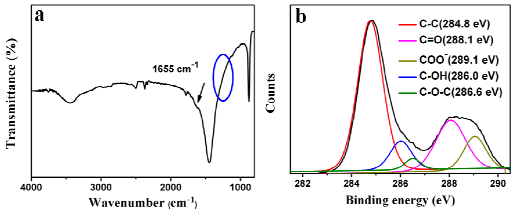

Figure. 5 FTIR (a) and C1s XPS (b) spectra of MCF GQDs in pH 13 solution.

On the basis of the results presented above, the local structure responsible for the special red PL of MCF GQDs was confirmed by density functional theory calculations (B3LYP/6-31G*). The main geometric parameters (Å) for ground and excited structures are shown in Figure 6a and 6b. It is notable that Na atom in COONa is also bounded to O atom in C=O of quinone structure. The HOMO (Figure 6c) and LUMO (Figure 6d) energy gaps of ground and excited structures of one luminescent unit obtained from theoretical calculation are -5.37 and -2.70 eV, respectively. The calculated absorption wavelength is at 532 nm with an oscillator strength of 0.165, and the corresponding PL wavelength is 632 nm with an oscillator strength of 0.142 (Figure 6 and Table S2), which is very close to the experimentally measured 625 nm. This is also confirmed from the change of C=C bond length from 1.388 to 1.441 Å (Figure 6a, 6b).

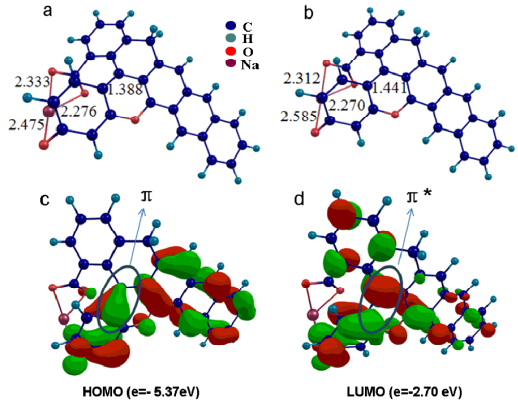

Figure. 6 The main geometric parameters (Å) for ground (a) and excited (b) structures, HOMO (c) and LUMO (d) energy gaps of ground and excited structures of one luminescent unit of MCF GQDs responsible for the red fluorescence color obtained from theoretical calculation with density function theory calculations (B3LYP/6-31G*).

The optimized local structure of MCF GQDs from lactone to quinone structure in strong alkaline condition is shown in Figure 7a and 7b. The former is composed of hydroxy, epoxy, and lactone groups which are generated by numerous tertiary alcohols reacting with nearby carboxylic acids on the periphery of GQDs. The later is associated with the red PL, which arises from the quinone structures transformed from the lactone ring opened in strong alkaline condition. The structural model of MCF GQDs in neutral and strong alkaline conditions is shown in Figure 7c and 7d. The strong red luminescence from the GQDs is emitted by a high concentration of modified quinone structures chemically linked to the GQDs after absorption through the graphene π–π* and n–π* transitions. Such GQDs stand out of the acid-base indicator phenolphthalein (no fluorescence could be observed in phenolphthalein) by the unique feature that the light absorbers and the robust structural base is the graphene

Nanoscale Accepted Manuscript

This journal is © The Royal Society of Chemistry 2015

Please do not adjust margins

framework modified with quinone structures, giving rise to the red PL with excellent stability when maintaining pH at about 12 to 14.

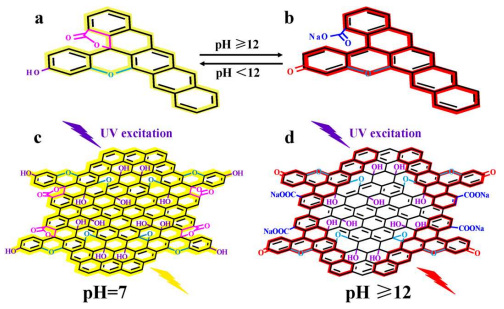

Figure. 7 Schematic representation of local structural transformation of MCF GQDs from lactone (a) to quinone (b) modeled by theoretical calculation. The structural model of MCF GQDs in neutral (c) and strong alkaline (d) conditions.

To verify that the quinone structures of GQDs were coming from their lactone structures in the strong alkaline condition, control experiments were carried out. When the GQDs solution at pH 7 were first reduced by $NaBH_4$ at 75 °C for 2 h (called rGQDs), the strong blue fluorescence instead

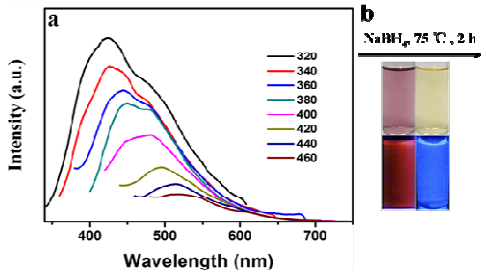

Figure. 8 (a) The fluorescence spectra of rGQDs in strong alkaline condition. (b) The appearance color under daylight (above) and fluorescence color under UV light (below) of MCF GQDs (left) and rGQDs (right) in alkaline condition.

of red fluorescence was observed in alkaline condition (Figure 8), and the appearance color was light yellow at pH 13 rather than red-brown (Figure 8b). As reported, $NaBH_4$ can apparently eliminate the lactone in graphene,[29] which indicates that the red PL must be associated with the quinone structures transformed from the lactone structures in MCF GQDs in the strong alkaline condition.

In terms of the MCF GQDs synthesis, two facets of control have been believed to lead to achieve a strong MCF GQDs aqueous solution. First, the electrochemical method facilitates the preparation of thin and small sized graphene sheets with a high amount of oxygen functionalities and associated charges, which conduces to the controlled reaction of groups at the edge of GQDs later. Second, refluxing the resulting powder from electrolysis in concentrated nitric and sulfuric acid mixed solution at certain temperature plays a vital role in generating large number of lactone groups by facilitating the reaction between tertiary alcohols and nearby carboxylic acids. When the reflux temperature was tuned from 80 to 100 and 140 °C, the average diameter about 10.6, 4.9, 2.8 nm could be obtained, and emitted strong orange-yellow, yellow-green and green fluorescence at pH 7, respectively (Figure S11, S12) (when the temperature was lower than 80 °C, *e.g.*, 60 °C, almost no fluorescence could be observed). However, despite different color due to different size at pH 7, upon raising pH > 11, these two GQDs solutions (at 100 and 140 °C) both emitted similar strong red fluorescence (Figure S13) to that at 80 °C, indicating that these three different sized GQDs share the same origin of the red fluorescence in the strong alkaline condition. On the other hand, if the graphite powder were refluxed in nitric and sulfuric acid mixed solution at 120 °C for 24 h but without the electrolysis procedure, no obvious red fluorescence color could be observed although a very weak emission peak at 622 nm presented in very strong alkaline condition (Figure S14). This clearly demonstrates that the small and thin GQDs with numerous lactone groups were obtained by the electrolysis of graphite and further reaction are critical for the generation of MCF GQDs at different pH conditions.

Measuring cellular temperature can help to explain intricate biological processes and to develop novel diagnoses.[30] The water soluble, all-pH range pH responsive MCF GQDs, coupled with their durability and biological compatibility are compelling and have prompted us to explore their potential in the thermoresponse. Therefore, it would be expected that the fluorescence properties of the novel MCF GQDs could be tuned by changing the pH as well as temperature. The fluorescence spectra of MCF GQDs in neutral condition in the temperature range 10-80 °C are shown in Figure 9a. With an increasing temperature, the intensity of fluorescence ideally exhibits a monotonous decrease with a good linear relationship in a wide temperature range. This could be attributed to the thermal activation of surface trap / defect states as well as to a thermally-induced increase in the nonradiative excitation recombination probability which are often observed in semiconductor quantum dots, and core-shell structured quantum dots.[31,32] The fluorescence spectrum of MCF GQDs was almost completely recoverable in a heating–cooling cycle between 10 and 80 °C (Figure 9b). The reversible process in the temperature range 10-80 °C can be readily repeated up to 6 cycles (Figure 9c) with a relatively slight decrease in the PL intensity. Moreover, as shown in Figure 9d, the emission intensity as a function of temperature at different pH condition exhibits a good linear relationship, indicating its potential application as dual sensing probe for highly sensitive reversible fluorescence response to pH value and temperature simultaneously (Figure S15).[1,33,34]

Nanoscale Accepted Manuscript

Please do not adjust margins

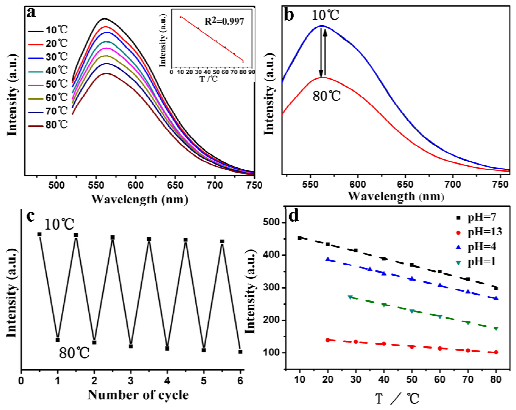

Figure. 9 Fluorescence spectra of MCF GQDs at neutral condition in the temperature range of 10-80 ℃ (inset: the emission intensity as a function of temperature) (a) and at the two temperatures 10 and 80 ℃ for heating-cooling cycle experiments (b). (c) The reversible fluorescence response curve over six consecutive heating-cooling cycles between 10 and 80 ℃. (d) The emission intensity of MCF GQDs as a function of temperature in different pH conditions.

Hela cells were used as a model to check that MCF GQDs could image the cells at different pH and temperatures. The cellular internalization of the MCF GQDs was investigated at different predetermined pH and temperature conditions. After incubating for 24 h (37°C, 5% CO_2, in Dulbecco's modified Eagle's medium (DMEM)), the culture medium was replaced by DMEM high glucose containing the MCF GQDs at predetermined pH value or temperature and further incubated for 2 h at 37°C. In order to equilibrate intracellular pH values, 10^{-6} g/ml nigericin and Britton-Robinson buffer solution with pH at 5, 7, 9 was added for 30 min to allow a rapid exchange of K^+ and H^+ which resulted in a rapid equilibration of external and internal pH values. Finally, the Hela cells were analyzed by confocal laser scanning microscopy. As the results shown in Figure 10, pH-induced fluorescence changes can be clearly observed. The fluorescence color red shift obviously from light yellow to dark orange with increasing cell culturing pH value from 5 to 9, in good agreement with the results obtained above. Meanwhile, the fluorescence signal of the MCF GQDs decreased as increasing the temperature from 24 °C to 40 °C in Hela cells (Figure S16), demonstrating the MCF GQDs in cells augurs well for practical applications in bioimaging and clinical diagnosis.[35]

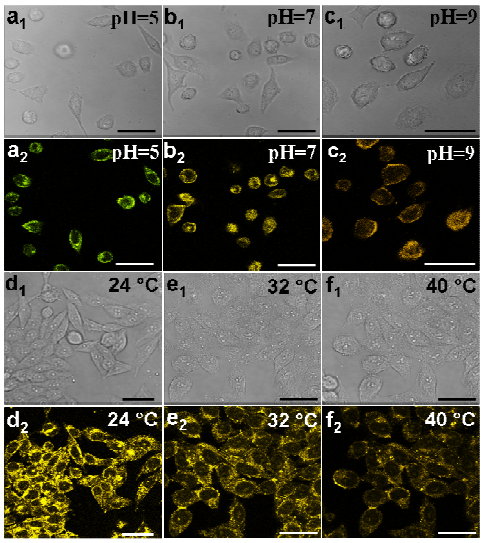

Figure. 10 Cell imaging of Hela cells at predetermined pH and temperature conditions (excitation at 405 nm). Bright field (a_1, b_1, c_1) and fluorescence field (a_2, b_2, c_2) of Hela cells cultured at predetermined pH value. Bright field (d_1, e_1, f_1) and fluorescence field (d_2, e_2, f_2) imaging of Hela cells at predetermined temperatures.

Formatted: Font color: Black

Conclusions

In summary, we have successfully prepared water-soluble, all-pH responsive, multicolor fluorescent graphene quantum dots (MCF GQDs) by electrochemical exfoliation of graphite followed by refluxing the resulting powder in concentrated nitric and sulfuric acid mixed solution. The colorimetric change at different pH from 1 to 14 can be easily perceived with the naked eye under ultraviolet lamp. We have demonstrated for the first time that the novel red PL results from the quinone structures transformed from the lactone structure in strong alkaline condition. To our knowledge, this is the first time such all-pH responsive GQDs indicators are invented and the root molecular structure elaborated. The PL of MCF GQDs was also found to respond to temperature changes, rendering the GQDs an ideal candidate of dual sensing probe for sensitive, reversible fluorescence response to pH value and temperature for bioimaging applications. Detailed follow-up work is underway in our laboratory and will be reported in due course.

Acknowledgements

This work is supported by NSFC (21073018), the Major Research Plan of NSFC (21233003), the Fundamental Research Funds for the Central Universities, Key Laboratory of Theoretical and Computational Photochemistry and RGC of Hong Kong (GRF No. 606511).

Nanoscale Accepted Manuscript

This journal is © The Royal Society of Chemistry 2015

Please do not adjust margins

Notes and references

1 C. Pietsch, R. Hoogenboom, U. S. Schubert, *Angew. Chem. Int. Ed.* 2009, **48**, 5653-5656.
2 Z. T. Fan, Y. C. Li, X. H. Li, L. Z. Fan, S. X. Zhou, D. C. Fang, S. H. Yang, *Carbon* 2014, **70**, 149-156.
3 Y.-P. Sun, B. Zhou, Y. Lin, W. Wang, K. A. S. Fernando, P. Pathak, M. J. Meziani, B. A. Harruff, X. Wang, H. Wang, P. G. Luo, H. Yang, M. E. Kose, B. Chen, L. M. Veca, S.-Y. Xie, *J. Am. Chem. Soc.* 2006, **128**, 7756-7757.
4 M. Zhang, L. Bai, W. Shang, W. Xie, H. Ma, Y. Fu, D. Fang, H. Sun, L. Fan, M. Han, C. Liu, S. Yang, *J. Mater. Chem.* 2012, **22**, 7461-7467.
5 X. Y. Tan, Y. C. Li, X. H. Li, S. X. Zhou, L. Z. Fan, S. H. Yang, *Chem. Commun.* 2015, **51**, 2544-2546.
6 Z. T. Fan, S. H. Li, F. L. YUAN, L. Z. Fan, *RSC Adv.* 2015, **5**, 19773-19789.
7 S. H. Li, Y. C. Li, J. Cao, J. Zhu, L. Z. Fan, X. H. Li, *Anal. Chem.* 2014, **86**, 10201−10207.
8 G. E. LeCroy, S. K. Sonkar, F. Yang, L. M. Veca, P. Wang, K. N. Tackett, J. J. Yu, E. Vasile, H. J. Qian, Y. M. Liu, *ACS Nano* 2014, **8**, 4522-4529.
9 J. Kim, J. S. Suh, *ACS Nano* 2014, **8**, 4190-4196.
10 L. B. Tang, R. B. Ji, X. M. Li, G. X. Bai, C. P. Liu, J. H. Hao, J. Y. Lin, H. X. Jiang, K. S. Teng, Z. B. Yang, *ACS Nano* 2014, **8**, 6312-6320.
11 H. J.Sun, N. Gao, K. Dong, J. S. Ren, X. G. Qu, *ACS Nano* 2014, **8**, 6202-6210.
12 X. F. Jia, J. Li, E. K. Wang, *Nanoscale* 2012, **4**, 5572-5575.
13 J. Peng, W. Gao, B. K. Gupta, Z. Liu, R. Romero-Aburto, L. Ge, L. Song, L. B. Alemany, X. Zhan, G. Gao, S. A. Vithayathil, B. A. Kaipparettu, A. A. Marti, T. Hayashi, J.-J. Zhu, P. M. Ajayan, *Nano Lett.* 2012, **12**, 844-849.
14 D. Pan, L. Guo, J. Zhang, C. Xi, Q. Xue, H. Huang, J. Li, Z. Zhang, W. Yu, Z. Chen, Z. Li, M. Wu, *J. Mater. Chem.* 2012, **22**, 3314-3318.
15 D. Pan, J. Zhang, Z. Li, M. Wu, *Adv. Mater.* 2010, **22**, 734-738
16 D. Pan, J. C. Zhang, Z. Li, C. Wu, X. M. Yan, M. H. Wu, *Chem. Commun.* 2010, **46**, 3681-3683
17 S. J. Zhu, J. H. Zhang, X. Liu, B. Li, X. F. Wang, S. J. Tang, Q. N. Meng, Y. F. Li, C. Shi, R. Hu, B. Yang, *RSC Adv.* 2012, **2**, 2717-2720.
18 S. H. Jin, D. H. Kim, G. H. Jun, S. H. Hong, S. Jeon, *ACS Nano* 2013, **7**, 1239-1245.
19 S. J. Zhu, J. H. Zhang, S. J. Tang, C. Y. Qiao, L. Wang, H. Y. Wang, X. Liu, B. Li, Y. F. Li, W. L. Yu, X. F. Wang, H. C. Sun, B. Yang, *Adv. Funct. Mater.* 2012, **22**, 4732-4740.
20 Y. Li, Y. Hu, Y. Zhao, G. Shi, L. Deng, Y. Hou, L. Qu, *Adv. Mater.* 2011, **23**, 776-780.
21 Y. Li, Y. Zhao, H. H. Cheng, Y. Hu, G. Q. Shi, L. M. Dai, L. T. Qu, *J. Am. Chem. Soc.* 2012, **134**, 15-18.
22 J.-L. Chen, X.-P. Yan, *Chem. Commun.* 2011, **47**, 3135-3137.
23 L. Minati, G. Speranza, I. Bernagozzi, S. Torrengo, L. Toniutti, B. Rossi, M. Ferrari, A. Chiasera, *J. Phys. Chem. C* 2010, **114**, 11068-11073.
24 M. S. Strano, C. B. Huffman, V. C. Moore, M. J. O'Connell, E. H. Haroz, J. Hubbard, M. Miller, K. Rialon, C. Kittrell, S. Ramesh, R. H. Hauge, R. E. Smalley, *J. Phys. Chem.B* 2003, **107**, 6979-6985.
25 C.-M. Popescu, B. C. Simionescu, *Applied Spectroscopy* 2013, **67**, 606-613.
26 K. K. Kunimoto, H. Sugiura, T. Kato, H. Senda, A. Kuwae, K. Hanai, *Spectroc. Acta Pt, A-Molec. Biomolec. Spectr.* 2001, **57**, 265-271.
27 Z. R. Yue, W. Jiang, L. Wang, S. D. Gardner, C. U. Pittman, *Carbon* 1999, **37**, 1785-1796.
28 H. P. Boehm, *Carbon* 2002, **40**, 145-149.
29 W. Gao, L. B. Alemany, L. J. Ci, P. M. Ajayan, *Nat.Chem.* 2009, **1**, 403-408.
30 J. Lee, N. A. Kotov, *Nano Today* 2007, **2**, 48-51.
31 L. M. Maestro, C. Jacinto, U. R. Silva, F. Vetrone, J. A. Capobianco, D. Jaque, J. G. Sole, *Small* 2011, **7**, 1774-1778.
32 L. M. Maestro, E. M. Rodriguez, F. S. Rodriguez, M. C. I. la Cruz, A. Juarranz, R. Naccache, F. Vetrone, D. Jaque, J. A. Capobianco, J. G. Sole, *Nano Lett.* 2010, **10**, 5109-5115.
33 J. M. Yang, H. Yang, L. W. Lin, *ACS Nano* 2011, **5**, 5067-5071.
34 L. Y. Yin, C. S. He, C. S. Huang, W. P. Zhu, X. Wang, Y. F. Xu, X. H. Qian, *Chem. Commun*. 2012, **48**, 4486-4488.
35 Y. Y. Li, H. Cheng, J. L. Zhu, L. Yuan, Y. Dai, S. X. Cheng, X. Z. Zhang, R. X. Zhuo, *Adv. Mater.* 2009, **21**, 2402-2406.

Nanoscale Accepted Manuscript